Materials Transactions, Vol. 48, No. 11 (2007) pp. 2945 to 2952

Density and Hardness Gradients of Functionally Graded Material Ring Fabricated from Al-3 mass%Cu Alloy by a Centrifugal *In-Situ* Method

Yoshimi Watanabe[1,2], Hisashi Sato[1,3], Tetsuro Ogawa[4] and Ick-Soo Kim[4]

[1]*Omohi College, Nagoya Institute of Technology, Nagoya 466-8555, Japan*
[2]*Department of Engineering Physics, Electronics and Mechanics Graduate School of Engineering, Nagoya Institute of Technology, Nagoya 466-8555, Japan*
[3]*Department of Techno-Business Administration Graduate School of Engineering, Nagoya Institute of Technology, Nagoya 466-8555, Japan*
[4]*Department of Functional Machinery and Mechanics Shinshu University, Ueda 386-8567, Japan*

In present study, the Al-Al_2Cu functionally graded material (FGM) ring was fabricated from Al-3 mass%Cu initial master alloy by the centrifugal *in-situ* method. In the case of Al-3 mass%Cu alloy, the density of the primary α-Al crystal is larger than that of the molten Al alloy. Therefore, the solid α-Al phase migrates towards the outer periphery of the ring when the centrifugal force is applied in the early stage of solidification. Consequently, since the Cu concentration within the FGM ring monolithically increases towards the ring's inner position, the FGM ring, whose density increases toward inner region, can be successfully fabricated by the centrifugal *in-situ* method from dilute Al-Cu alloy. It is also found that the hardness increases towards the inner region of the ring within the Al-Al_2Cu FGM ring. The hardness of the fabricated specimens at the inner region of the ring increases in a large scale by the heat treatments, since Guinier-Preston (GP) zones would be formed by aging. [doi:10.2320/matertrans.MB200710]

(Received February 27, 2007; Accepted August 6, 2007; Published September 12, 2007)

Keywords: *functionally graded material (FGM), density, solidification, viscosity, aluminum-copper alloy, Al_2Cu*

1. Introduction

A functionally graded material (FGM) is usually a combination of two materials that has a compositional gradient from one material at one surface to another material at the opposite surface. This compositional gradient allows the creation of multiple properties without any mechanically weak interface. It is possible with these materials to obtain a combination of properties that cannot be achieved in conventional materials. This makes FGMs preferable in many applications.[1,2)]

A variety of methods have been explored in attempts to fabricate the FGMs,[1,2)] and one of them is centrifugal solid-particle method.[3–6)] In this method, a thick walled FGM ring can be fabricated from a mixture of molten metal and solid particles. The composition gradient is formed mainly from the difference in the centrifugal force produced by the difference in density between the molten metal and solid particles. The moving direction of the solid particles in the molten matrix is determined by the density difference between the molten metal and particles. If the density of solid particles is higher than that of molten matrix, the particles migrate toward outer region of the FGM ring during the centrifugal solid-particle method, and *vice versa*. For example, SiC[5)] and Shirasu (volcanic eruptions, main composition: SiO_2 and Al_2O_3)[7)] dispersed in Al matrix FGM rings have been fabricated by the centrifugal solid-particle method. During the processing of the centrifugal solid-particle method, SiC (density: 3.15 Mg/m^3) and Shirasu (density: 2 Mg/m^3) particles in molten Al (density at 700°C: 2.37 Mg/m^3) migrate toward the outer and the inner periphery of the FGM ring, respectively.

In the case of Al-SiC FGM ring fabricated by the centrifugal solid-particle method, since the volume fraction of SiC particles with higher density than Al matrix increases toward the outer region of the ring, the overall density of the FGM ring also increases toward this direction. On the other hand, the volume fraction of Shirasu particles, which density is smaller than that of Al, increases in the inner region of the ring, and then the overall density of the Al-Shirasu FGM ring increases toward the outer region of the ring. In this way, the density of the outer part of the FGM rings is larger than that of the inner part of the ring in nature. In our resent study, theoretical study on fabrication of FGM with density gradient by a centrifugal solid-particle method has been carried out.[8)] The graded distributions of the two kinds of solid spherical particles under applied centrifugal force are analyzed theoretically. It is shown that the FGM ring in which the density will increase toward interior region from the outer region can be fabricated by the centrifugal solid-particle method using a combination of large diameter particles with low density and small one with high density.[8)]

Meanwhile, there is another FGM ring fabrication method using the centrifugal force, namely a centrifugal *in-situ* method, by which the centrifugal force can be applied during the solidification to both the primary crystal and the matrix.[9–11)] This situation can be realized when the processing temperature is higher than the liquidus of the reinforcement materials in phase diagram. Usually, the density of the outer part of the FGM rings fabricated by the centrifugal *in-situ* method is larger than that of the inner part of the ring.

In many cases, the volume fraction of reinforcement particles increases towards the outer region of Al-based FGM rings, since the density of reinforcement particles is usually higher than that of the molten Al. Consequently, the hardness and wear resistance of Al based FGM ring fabricated by the centrifugal method increase towards the ring's outer region.[12,13)] When the inner region of the ring is required to

have high mechanical properties, the density of reinforcement particles should have a smaller value compared to that of the molten Al. However, the above systems are limited, and the mechanical properties of the lighter particle-reinforced FGM would not be strong. Therefore, a new approach is needed to fabricate an FGM ring, in which both density and mechanical property gradients increase towards the ring's inner region.

It is reported that the volume change accompanying the solidification of pure Al is 7.14%.[14] In the case of dilute Al alloys, the density of the primary α-Al crystal is larger than that of the molten Al alloy. If this system is used for the initial master alloy of the centrifugal *in-situ* method, the primary α-Al crystal particles should migrate towards the outer periphery of the ring. Then, an FGM ring, whose density would increase toward the inner region of the ring, can be fabricated by using this phenomenon.

To address this issue, we have used an Al-3 mass%Cu alloy as an initial material for the centrifugal *in-situ* method. As it will be described in the next section, since the density of the primary α-Al crystal is larger than that of a molten Al-3 mass% Cu alloy at early stage of solidification, primary α-Al solid particles migrate towards the outer periphery of the ring. The volume fraction of the precipitates of Al_2Cu intermetallic compound, which has higher density than α-Al phase, would increase towards the inner periphery of the ring. Then the density of the FGM ring should increase toward the ring inner region.

2. Density Change During Solidification of Al-3 mass%-Cu Alloy

The density difference between the primary crystal and retained molten alloy is one of the most important physical properties to understand the formation mechanism of graded microstructure within the FGM fabricated under the centrifugal force. In this section, we will describe first the density change during the solidification of the Al-3 mass% Cu alloy. Figure 1 shows the density of molten Al-Cu alloys at 600°C, 700°C, 800°C and 900°C, as well as that of a solid Al-Cu alloy at 20°C.[15] Dotted line in 600°C is an extrapolated line. It can be seen, the density of molten Al-Cu alloys increases with increasing the Cu concentration, and the density as a function of Cu concentration has a positive curvature.

Figure 2 presents the Al-Cu phase diagram.[16] When the Al-3 mass%Cu alloy is cooled from a temperature within the liquid-phase region, the solid α-Al phase begins to form at about 653°C and the chemical composition of primary α-Al phase is 0.5 mass%Cu in equilibrium. With continued cooling, the compositions of the liquid and α-Al phases follow the liquidus and solidus lines, respectively. For example, they are about 8.0 mass% Cu and 1.1 mass% Cu at 640°C and are about 14.4 mass% Cu and 2.1 mass% Cu at 620°C, respectively. The solidification process is complete at about 600°C. At just the above this temperature, the composition of the last remaining liquid Al-Cu alloy is about 20.0 mass% Cu, while that of the α-Al phase is approximately 3 mass%Cu.

Meanwhile, the density of a solid Al-Cu alloy at elevated temperature can be calculated by density and linear thermal expansion coefficient using eq. (1),

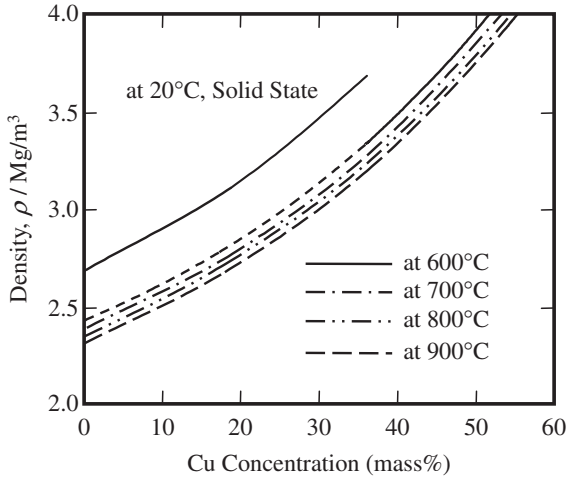

Fig. 1 Density of molten Al-Cu alloys at 600°C, 700°C, 800°C and 900°C, as well as that of a solid Al-Cu alloys at 20°C, after Bornemann and Sauerwald.[15]

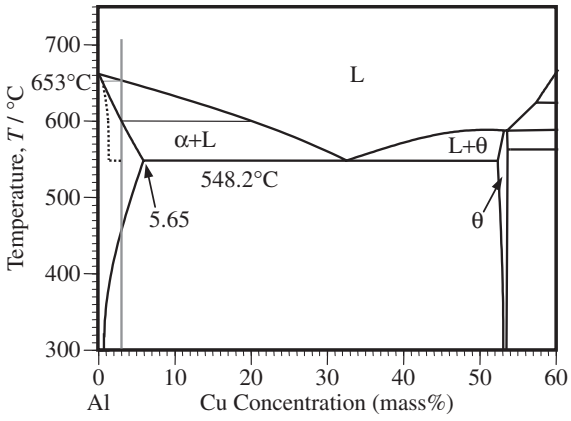

Fig. 2 The Al-Cu phase diagram.[16]

$$\rho_T = \frac{\rho_0}{(1+\alpha\Delta T)^3} \tag{1}$$

where ρ_T, α, ΔT and ρ_o are density at temperature T, linear thermal expansion coefficient, temperature change and density at base temperature, respectively. It is known that the thermal expansion coefficient of pure Al at 27°C, 327°C and 527°C is $23.2 \times 10^{-6}\,K^{-1}$, $28.4 \times 10^{-6}\,K^{-1}$ and $34.0 \times 10^{-6}\,K^{-1}$, respectively.[17] Using these values, the density of solid α-Al in Al-Cu system at elevated temperature can be evaluated. During infinitely slow (equilibrium) solidification, the density change for liquid and solid phases during the cooling of molten Al-3 mass% Cu alloy is shown in Fig. 3.

In case of centrifugal casting, however, solidification without diffusion may take place in the solid but the liquid composition is always kept homogeneous during solidification due to an efficient stirring. The composition of the liquid, C_L, during solidification is given by the Scheil equation,

$$C_L = C_0(1-f_s)^{k-1} \tag{2}$$

where C_0, k and f_s are the initial composition, the equilibrium distribution coefficient and the mass friction of solid, respectively.[18] Assuming $C_0 = 3.0$ and $k = 0.17$, the solid-

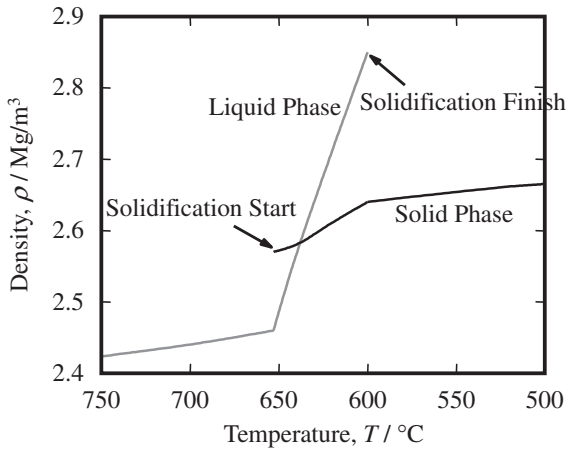

Fig. 3 Temperature dependence of densities for liquid and solid phases during the infinitely slow (equilibrium) solidification of molten Al-3 mass% Cu alloy.

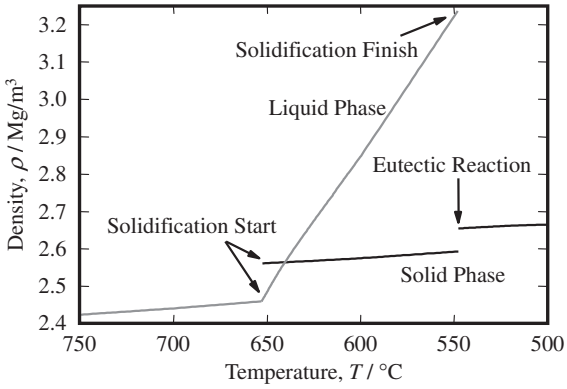

Fig. 4 Temperature dependence of densities for liquid and solid phases during the cooling of molten Al-3 mass% Cu alloy. Solidification without diffusion may take place in the solid but the liquid composition is always kept homogeneous during solidification due to an efficient stirring.

ification process is not complete at 600°C, at which the composition of the liquid phase becomes 20 mass% Cu, and the fraction of liquid phase is about 10%. Even at a eutectic temperature, 5.5% liquid phase with the eutectic composition will be retained. The retained liquid phase may transform into the solid phases by the eutectic reaction at this temperature. The mean composition of the solid $\overline{C}$s will be purer than that of the equilibrium solidus line, when there is no diffusion in the solid. When f_s calculated from C_L is V_s, $\overline{C}$s at C_L can be calculated by the integration of Scheil equation from 0 to V_s and the division with V_s,

$$\overline{C\mathrm{s}} = \frac{1}{V_\mathrm{s}} \int_0^{V_s} kC_0(1-f_\mathrm{s})^{k-1} df_\mathrm{s} = \frac{C_0}{V_\mathrm{s}}\{1-(1-V_\mathrm{s})^k\}. \quad (3)$$

In this study, V_s for each C_L are calculated by eq. (2) and liquidus line in equilibrium state. Then non-equilibrium solidus line ($\overline{C}$s) are evaluated by eq. (3) and V_s calculated from eq. (2). The obtained result is shown in Fig. 2 by a dotted line.

For solidification without diffusion in the solid but with perfect mixing in the liquid, the density change for liquid and solid phases can be also calculated. Figure 4 shows the result for Al-3 mass% Cu alloy. It can be seen that the density of the liquid phase slightly increases with decreasing the temperature before the solid α-Al phase begins to form at about 653°C, since the chemical composition of liquid phase maintains constant (*i.e.*, 3 mass%Cu). On the other hand, the density of liquid phase increased rapidly below 653°C. This is because the composition of the liquid phase follows the liquidus line, as shown in Fig. 2. Temperature dependence of density for solid phase during the solidification is relatively small comparing with liquid phase, since the composition change during the solidification is small (from 0.5 mass% Cu to 1.3 mass% Cu). It must be noted that the density of the primary α-Al crystal with 0.5 mass% Cu is larger than that of a molten Al-3 mass% Cu alloy at 653°C. Therefore, in the early stage of solidification, solid α-Al phase migrates towards the outer periphery of the ring when the centrifugal force is applied. The volume fraction of the Al_2Cu intermetallic compounds would increase towards the inner periphery of the ring. Consequently, the density and hardness will increase toward inner region of the ring, since the density and hardness of the Al_2Cu intermetallic compounds are larger than those of the α-Al.

3. Experimental Procedures

Al-Al_2Cu FGM ring was fabricated by the centrifugal *in-situ* method from Al-3 mass%Cu initial master alloy. The alloy was melted in an argon gas atmosphere at 800°C. Only liquid phase exists in Al-3 mass%Cu alloy at 800°C. The molten alloy was directly poured into a rotating mold, which was heated to 750°C. The applied G number was 120, where the G number is the centrifugal force in units of gravity.[3,4] The ratio of the centrifugal force to the gravity (g) is given by the following equation:

$$G = \frac{F}{g} = \frac{2\pi DN^2}{g} \quad (4)$$

where F (N), D (m) and N (s^{-1}) are a centrifugal force, a diameter of the cast ring and the velocity of the mold rotation, respectively. After casting, the mold was cooled in air. The fabricated ring had the outer diameter of 90 mm, the thickness of about 20 mm and the length of 30 mm.

Specimens for scanning electron microscopy (SEM) were cut from the cast ring and prepared by grinding and polishing. The specimens were examined in a Hitachi 3000 SEM equipped with electron-dispersive X-ray spectroscope (EDX). Density distribution of fabricated FGM ring was evaluated by means of Archimedes type density test at different positions. The fabricated specimen was divided into five parts of equal width along the centrifugal force direction, and density of each sample was measured. Brinell hardness test and micro Vickers hardness test were carried out to study the gradient of the mechanical property. In the present study, load and pressing for Brinell hardness test were 4900 N and 30 sec, respectively, whereas those for the micro Vickers hardness test were 1.96 N and 15 sec, respectively.

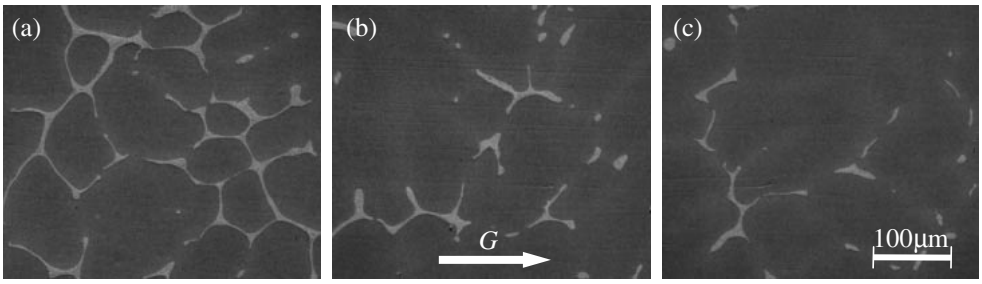

Fig. 5 The typical SEM microstructures of the Al-Al_2Cu FGM ring. The arrow indicates the direction of the centrifugal force. (a) ring's inner region, (b) ring's interior region, (c) ring's outer region.

The effect of heat treatment on the hardness is also studied. To avoid the compositional gradient change due to the diffusion during the heat treatments, the fabricated FGM ring was cut into smaller samples. The smaller samples were encapsulated in an evacuated quartz tubes, and the heat treatments were carried out in a muffle furnace. The samples were heated at 550°C for 20 h, and then quenched into water (solution treatment). Some of these solution treatment samples were aged at 160°C for 8 h. X-ray diffraction (XRD) analysis was carried out for the samples before and after the heat treatments.

4. Results

4.1 Microstructures

Figure 5 shows the typical microstructures of the Al-Al_2Cu FGM ring fabricated from Al-3 mass%Cu alloy by the centrifugal *in-situ* method, where (a), (b) and (c) were taken at ring's inner, ring's interior and ring's outer regions, respectively. In this figure, an arrow indicates the direction of the centrifugal force. White phase is identified by EDX analysis to be the Al_2Cu intermetallic compound and black regions are α-Al. White regions in these figures have a eutectic microstructure. Eutectic, which is formed in the final stage of solidification, is distributed in the grain boundary regions. The volume fraction of the eutectic can be evaluated using the Scheil equation, and that is 5.5%, which is in a good agreement with experimental observations. It is found that the volume fraction of Al_2Cu phase increases towards the ring's inner position (opposite the centrifugal force direction). This is because the α-Al primary crystal particles migrate towards the outer periphery of the ring under the application of the centrifugal force, since the density of the α-Al primary crystal is larger than that of the molten Al-Cu alloy in the early stage of solidification. The volume fraction of Al_2Cu intermetallic compound, therefore, increases towards the inner region of the ring.

In order to express the Cu concentration gradation in the α-Al matrix quantitatively, the distribution of the Cu concentration in the FGM ring was measured by EDX analysis. Results are shown in Fig. 6, where the abscissa represents the position normalized by thickness of the ring; *i.e.* 0.0 is the inner surface and 1.0 is the outer surface. As it can be seen, the Cu concentration monotonically increases towards the ring's inner position. It was quantitatively confirmed that the Cu concentration increases towards the inner periphery of the ring.

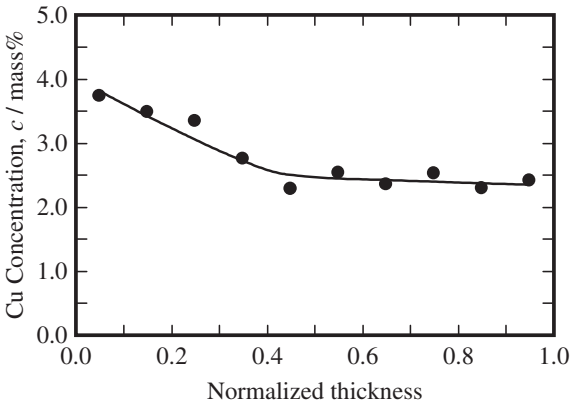

Fig. 6 Distribution of the Cu concentration in the Al-Al_2Cu FGM ring measured by EDX analysis.

4.2 Heat treatment

Precipitation hardening is commonly employed with high-strength Al alloy. The mechanism of hardening has been studied most extensively for the Al-Cu alloys. Therefore, in this study, the smaller samples of fabricated FGM are heat-treated. Although the figure is not presented here, it was found that the Al_2Cu intermetallic compound could not be found after heat treatments (both solution treatment and aging). The Al_2Cu will disappear by solution treatment and not form by precipitation during aging.

To discuss the above phenomenon, XRD analysis was carried out. Figures 7(a), (b) and (c) show the XRD patterns of sample, which is cut from an inner region of the FGM ring, before and after the solution treatment and aging, respectively. It is seen that the Al and the Al_2Cu peaks co-exist before the heat treatments. Alternatively, the Al_2Cu peaks disappear and only the Al peaks were found after the solution treatment. Moreover, the Al_2Cu peaks cannot be detected after aging, since the heat treatment was carried out at low temperature for short time. Hence, the supersaturated solid solution and Guinier-Preston (GP) zones would be formed after the solution treatment and the aging, respectively.

4.3 Density gradient

Figure 8 shows the distributions of the density measured by Archimedes method and the theoretically calculated density. The theoretical density was calculated from Cu concentration in Al-Al_2Cu FGM ring shown in Fig. 6. As shown in Fig. 2, Cu solubility in α-Al phase at 300°C is 0.68 mass%Cu.[16] On the other hand, Löchte *et al.* have

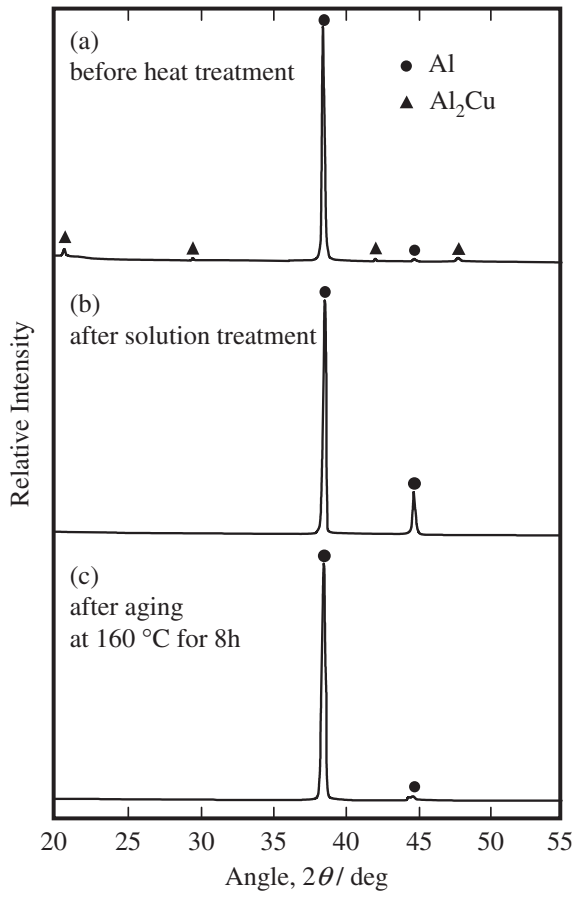

Fig. 7 XRD patterns of the FGM ring. (a): Before the heat treatments, (b): After the solution treatment and (c): After the aging at 160°C for 8 h.

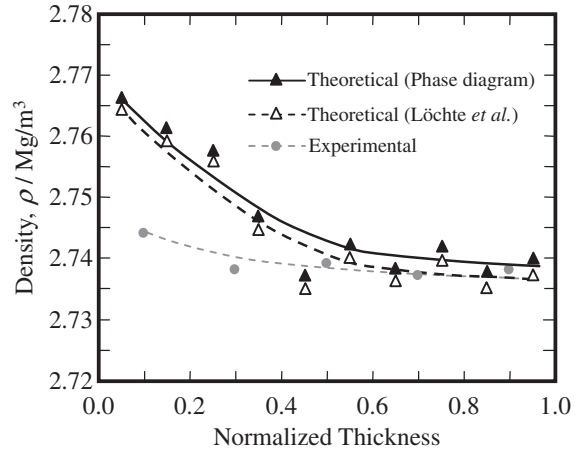

Fig. 8 Distributions of the measured and calculated densities in the Al-Al_2Cu FGM ring.

reported that Cu solubility below 200°C is less than 0.1 at.%Cu (0.24 mass%Cu).[19] From these Cu solubility, Cu concentration used for the formation of Al_2Cu phase at 300°C or below 200°C are 0.68 mass% or 0.24 mass% less than Cu composition shown in Fig. 6, respectively. Densities of Al-0.68 mass%Cu alloy and Al-0.24 mass%Cu alloy can be estimated as 2.706 Mg/m^3 and 2.695 Mg/m^3 from Fig. 1, respectively. On the other hand, density of Al_2Cu phase is

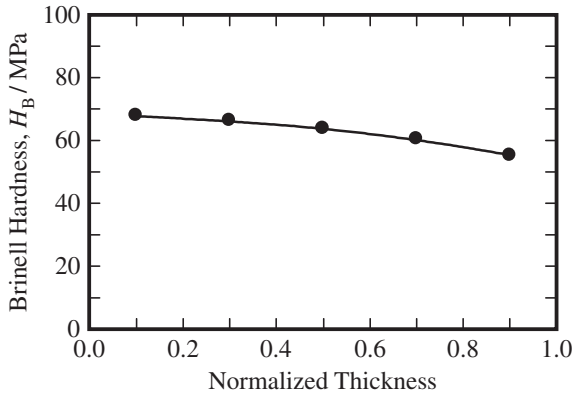

Fig. 9 Distribution of the Brinell hardness in the Al-Al_2Cu FGM ring before heat treatment.

4.4 Mg/m^3. Using these densities, volume fraction of Al_2Cu phase can be obtained from the Cu concentration. The densities of Al-Cu alloy calculated from the volume fraction of Al_2Cu phase were plotted as theoretical densities in Fig. 8. Closed and open triangular plots show theoretical densities calculated using Cu solubility of 0.68 mass% at 300°C and 0.24 mass% below 200°C, respectively. As can be seen from this figure, the density of Al-Al_2Cu FGM ring increases toward the inner region of the ring. In this way, the Al-Al_2Cu FGM ring that has density gradient toward inner region can be successfully fabricated by the centrifugal method from dilute Al-Cu alloy. As mentioned above, the volume fraction of Al_2Cu intermetallic compound increases toward the ring's inner position. Therefore, the density increases toward the inner region of the ring, since the density of Al_2Cu (4.4 Mg/m^3) is larger than that of pure Al (2.7 Mg/m^3). Also, the theoretical densities calculated from Cu concentration are good agreed with the density measured by Archimedean method.

4.4 Hardness Gradients

In order to study the gradient of the mechanical property, hardness tests were performed. It was shown that the Al-Al_2Cu FGM ring without heat treatment has dual-phase structure (Al and Al_2Cu), and the coarser primary α-Al and Al/Al_2Cu eutectic microstructure was found (Fig. 5). Therefore, measuring hardness by using a small indenter was not the best method to evaluate the hardness of the whole specimen. In the present study, the Brinell hardness test with a large indenter, whose diameter is 10 mm, was adopted. In contrast, the FGM after heat treatments had quasimono-phase structure with the very fine microstructure. The micro Vickers hardness test was, therefore, carried out on the heat-treated specimens, since the detailed hardness distributions could be obtained.

The distribution of the Brinell hardness in the Al-Al_2Cu FGM ring before heat treatment is shown in Fig. 9. As it can be seen, the Brinell hardness of the ring's inner region is larger than that of the ring's outer region. This is because the content of Al_2Cu intermetallic compound increases towards the ring's inner position, and the hardness of the Al_2Cu intermetallic compound is much larger than that of the Al. In this way, the Al-Al_2Cu FGM ring with hardness gradient can

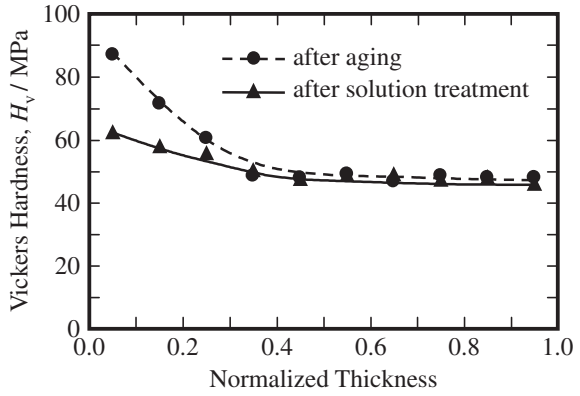

Fig. 10 Distributions of the micro Vickers hardness in the solution-treated specimen and in the aged specimen.

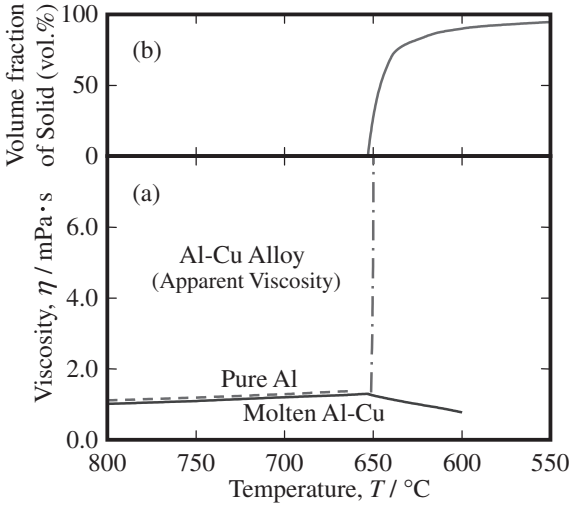

Fig. 11 (a) Temperature dependence of the viscosity and apparent viscosity for molten Al-Cu alloy during the solidification of Al-3 mass%Cu alloy, as well as that for pure Al. (b) Volume fraction of solid during the solidification of Al-3 mass%Cu alloy.

be successfully fabricated by the centrifugal *in-situ* method from dilute Al-Cu alloy, when the hardness increases towards the inner region of the ring.

Figure 10 shows the distributions of the micro Vickers hardness after solution-treatment and aging. It is apparent that a higher micro Vickers hardness value was found around in the inner region of the ring. The micro Vickers hardness of the specimens at inner region of the ring increases in a large scale by aging. Although there is no evidence, GP zones should be formed by aging.

5. Discussion

In this study, it was found that the Cu concentration within the FGM ring monotonically increases towards the ring's inner position as shown in Fig. 6. This may come from the α-Al particles migrate toward the outer region of the FGM ring under the centrifugal force, since the moving direction of the solid particles in the molten matrix could be determined by the density difference between the molten metal and particles. However, as shown in Fig. 4, the temperature dependence of the density for the solid phase is smaller than that for the liquid phase, and they are crossed at about 640°C. Therefore, while the density of the primary α-Al crystal is larger than that of a molten Al-Cu alloy at a temperature above about 640°C, the density of the primary α-Al crystal is smaller than that of a molten Al-Cu alloy below about 640°C. Since the primary α-Al crystals migrate toward the outer region of the FGM ring below about 640°C, non-monotonic gradation should be appeared within the fabricated FGM ring. This contradicts with the observed microstructure. In this section, we will discuss the formation of graded microstructure during the solidification under the centrifugal force.

During fabrication of the FGM ring by the centrifugal *in-situ* method, the particles in the molten metal behave as a suspension of hard particles in a viscous liquid. Therefore, the composition gradient formed by the centrifugal *in-situ* method can be affected by the viscosity of the melt, as well as the difference in density between particles and a molten metal, the applied G number, the particle size, the mean volume fraction of particles, and so on. During the solidification, the apparent viscosity of the melt (suspension) should be influenced by the temperature, Cu concentration and volume fraction of solid.

It is known that the relationship between liquid viscosity η (mPa·s) and temperature T (K) can be expressed by the Arrhenius' formula (Andrade's equation)

$$\eta = \mathrm{A}\exp(B/RT) \tag{5}$$

where R is the gas constant (= 8.3144 (J·mol^{-1}·K^{-1})) and A and B are constants.[20] Measured and calculated values of A and B in eq. (5) for pure Al reported by Hirai are 0.2565 and 0.244 (mPa·s) and 13.08 and 15.67 (kJ·mol^{-1}), respectively.[21] Using these values, temperature dependence of the viscosity of pure Al can be calculated, and results are shown in Fig. 11(a).

The effect of Cu concentration on the viscosity of molten Al-Cu alloy can be found in a literature.[22] There is a linear relationship between the Cu concentration and the viscosity when the alloy contains less than 20 mass%Cu. The viscosity of molten Al-20 mass%Cu alloy is a half value of that for the pure Al.[22] Therefore, the viscosity of molten Al-Cu alloy during the solidification of Al-3 mass%Cu alloy can be evaluated, and results are also shown in Fig. 11(a). As can be seen, the viscosity increases slightly with decreasing the temperature before solidification starts, since the chemical composition of molten Al-Cu is constant (Al-3 mass%Cu). After solidification starts, in contrast, the viscosity decreases with decreasing the temperature, since the chemical composition of the molten Al-Cu changes along the liquidus line, as shown in Fig. 2.

It is known that the viscosity of the melt increases according to the increase in number of particles in the suspension. Various equations have been proposed to predict the variation of the viscosity in the case of a relatively large volume fraction of particles.[23] Most useful is the Brinkmann equation,[24] which gives the apparent viscosity η as

$$\eta = \eta_0/(1 - V/V_{max})^{2.5} \tag{6}$$

where η_0 is the viscosity of the molten metal without

particles, V is the particle volume fraction and V_{max} is the maximum packing fraction. The V_{max} varies depending on the packing condition and the theoretical value is in the range of 0.52 for the simple cubic packing to 0.74 for the close packing of spherical particles.

To calculate the apparent viscosity of semi-solid alloy, the volume fraction of solid at each temperature is evaluated from Fig. 2 using the lever rule. Figure 11(b) shows the volume fraction of solid during the solidification of Al-3 mass%Cu alloy. Using this curve with eq. (6), apparent viscosity of Al-Cu alloy during the solidification of Al-3 mass%Cu alloy is calculated, and results are also shown in Fig. 11(a). It is important to note that the apparent viscosity sharply increases with decreasing the temperature after solidification starts. The following equation was reported for the apparent viscosity of Al-10 mass%Cu semi-solid alloy.[25)]

$$\eta = \eta_0 \left\{ 1 + \frac{2.41 \times 10^6 C^{1/3} \dot{\gamma}^{-4/3}}{2\left(\frac{1}{f_s} - \frac{1}{0.72 - 8.82 C^{1/3} \dot{\gamma}^{-1/3}} \right)^3} \right\} \quad (7)$$

where f_s, C and $\dot{\gamma}$ are mass friction of solid, average solidification rate (s^{-1}) and shear rate (s^{-1}), respectively. The apparent viscosity rapidly increases when the fraction of solid is more than about 0.5. This fact also supports our previous discussion.

Needless to say, the volume fraction of particles changes as the position on the ring changes. However, since the microstructural development during the centrifugal *in-situ* method is still not well understood,[11)] the position dependency of viscosity will not be discussed any more. As shown in Fig. 4, the temperature *vs* density curves for the solid and liquid phases are crossed at about 640°C, and the density of the primary α-Al crystal is smaller than that of a molten Al-Cu alloy below this temperature. However, at this temperature, since the volume fraction of particles is more than 70%, the apparent viscosity is extremely high. Therefore, migration of α-Al phase towards the innner periphery of the ring will not be occurred.

Thus, the formation of the graded composition in the FGM ring fabricated by the centrifugal *in-situ* method from Al-3 mass%Cu alloy could be summarized as follows. After the molten Al-Cu alloy is poured into a rotating mold, the α-Al primary crystals with 0.5 mass%Cu are crystallized. Since the density of the α-Al primary crystal (about 2.57 Mg/m^3) is larger than that of the molten Al-Cu alloy (about 2.46 Mg/m^3) at solidification temperature, the α-Al primary crystal particles will migrate toward the outer periphery of the ring. During the solidification (cooling), the densities difference between the molten Al-Cu alloy and α-Al primary crystal particles becomes smaller and it becomes zero at 640°C. However, at this time, volume fraction of solid is high enough, and the α-Al primary crystal particles cannot migrate any more. Therefore, α-Al primary crystal particles always migrate toward the outer periphery of the ring. Then, the remaining molten Al-Cu alloy will solidify. At a eutectic temperature, 5.5% liquid phase with a eutectic composition will be retained, and the retained liquid phase may transform into the solid phases by the eutectic reaction. By this means, the volume fraction of the Al_2Cu intermetallic compound increases toward the ring's inner position. The density should, therefore, increase toward the inner periphery of the ring, since the density of an Al_2Cu intermetallic compound (the density is 4.4 Mg/m^3) is larger than that of a pure Al (the density is 2.7 Mg/m^3). Moreover, the hardness of the ring's inner position becomes larger than that of the outer region, since the hardness of Al_2Cu intermetallic compound is larger than that of α-Al.

6. Conclusions

In present study, the Al-Al_2Cu FGM ring with the density and hardness gradients was fabricated from Al-3 mass%Cu initial master alloy by the centrifugal *in-situ* method. Based on the present study, the following conclusions were made.

(1) It is found that the Cu concentration within the FGM ring monolithically increases towards the ring's inner position.
(2) The Al-Al_2Cu FGM ring, whose density increases toward inner region, can be successfully fabricated by the centrifugal *in-situ* method from dilute Al-Cu alloy.
(3) It is found that the Al-Al_2Cu FGM ring with hardness gradient could be fabricated in which hardness increases towards the inner region of the ring.
(4) The hardness of the fabricated specimens at the inner region of the ring increases in a large scale by the heat treatments, since GP zones would be formed by aging.

Acknowledgements

The authors acknowledge the support of 21st Century COE Research by the Ministry of Education, Culture, Sports, Science and Technology of Japan and The Light Metal Educational Foundation Inc. of Japan for sponsoring the project. The authors also wish to thank Dr. Oleg Sitdikov for useful comments and suggestions on the manuscript.

REFERENCES

1) S. Suresh and A. Mortensen: *Fundamentals of Functionally Graded Materials, Processing and Thermomechanical Behavior of Graded Metals and Metal-Ceramic Composites*, (IOM Communications Ltd, London, 1998).
2) Y. Miyamoto, W. A. Kaysser, B. H. Rabin, A. Kawasaki and R. G. Ford (Eds.): *Functionally Graded Materials: Design, Processing and Applications*, (Kluwer Academic Publishers, Boston, 1999).
3) Y. Fukui: JSME Inst. J. Series III **34** (1991) 144–148.
4) Y. Watanabe, N. Yamanaka and Y. Fukui: Composites Part A **29A** (1998) 595–601.
5) Y. Fukui and Y. Watanabe: Metal. Mater. Trans. A **27A** (1996) 4145–4151.
6) Y. Watanabe, A. Kawamoto and K. Matsuda: Comp. Sci. Tech. **62** (2002) 881–888.
7) Z. M. Salim, N. Yamanaka, Y. Watanabe, Y. Fukui and S. Nunomura: *ADVANCED MATERIALS AND PROCESSING" vol. 2, Proceedings of the 2nd Pacific Rim International Conference on Advanced Materals and Processing (PRICM-2)*, (The Korean Institute of Metals and Materials, 1995) pp. 1739–1744.
8) T. Ogawa, Y. Watanabe, H. Sato, I.-S. Kim and Y. Fukui: Composites Part A **37A** (2006) 2194–2200.
9) Y. Fukui, K. Takashima and C. B. Ponton: J. Mater. Sci. **29** (1994) 2281–2288.
10) Y. Watanabe, R. Sato, K. Matsuda and Y. Fukui: Sci. Eng. Comp.

Mater. **11** (2004) 185–199.
11) Y. Watanabe and S. Oike: Acta Mater. **53** (2005) 1631–1641.
12) Y. Watanabe, N. Yamanaka, Y. Oya-Seimiya and Y. Fukui: Z. Metallkd. **92** (2001) 53–57.
13) Y. Watanabe and T. Nakamura: Intermetallics **9** (2001) 33–43.
14) P. J. Way: Met. Trans. **5** (1974) 2602–2603.
15) K. Bornemann and F. Sauerwald: Z. Metallk. **14** (1922) 145–159.
16) T. B. Massalski (ed): *Binary Alloy Phase Diagrams*, (ASM International, Materials Park, 1988).
17) Japan Society of Thermophysical Properties (Ed): *Thermophysical Properties Handbook*, (Yokendo, Tokyo, 1990) p. 22. (in Japanese).
18) D. A. Porter and K. E. Easterling: *Phase Transformations in Metals and Alloys*, (Van Nostrand Reinhold Company, New York, 1981), p. 209.
19) L. Löchte, A. Gitt, G. Gottstein and I. Hurtado: Acta Mater. **48** (2000) 2969–2984.
20) R. F. Brooks, A. T. Dinsdale and P. N. Quested: Meas. Sci. Technol. **16** (2005) 354–362.
21) M. Hirai: ISIJ Inter. **33** (1993) 251–258.
22) F. D. Richardson: *Physical Chemistry of Melts in Metallurgy, Volume 1*, (Academic Press, London and New York, 1974) p. 26.
23) H. L. Frisch and R. Simha: *The Viscosity of Colloidal Suspensions and Macromolecular Solutions, in "Rheology, Theory and Applications, vol. 1"* ed. by F. R. Eirich, (Polytechnic Institute of Brooklyn, New York, 1956), p. 525.
24) H. C. Brinkman: J. Chem. Phys. **20** (1952) 571–571.
25) M. Hirai, K. Takebayashi, Y. Yoshikawa and R. Yamaguchi: ISIJ Inter. **33** (1993) 405–412.